Rapid Assembly of Alzheimer-like Paired Helical Filaments from Microtubule-Associated Protein Tau Monitored by Fluorescence in Solution†

Peter Friedhoff, Anja Schneider, Eva-Maria Mandelkow, and Eckhard Mandelkow*

Max-Planck-Unit for Structural Molecular Biology, Notkestrasse 85, D-22607 Hamburg, Germany

Received March 9, 1998; Revised Manuscript Received April 23, 1998

ABSTRACT: Alzheimer's disease is characterized by the progressive deposition of two types of fibers in the affected brains, the amyloid fibers (consisting of the Aβ peptide, generating the amyloid plaques) and paired helical filaments (PHFs, made up of tau protein, forming the neurofibrillary tangles). While the principles of amyloid aggregation are known in some detail, the investigation of PHF assembly has been hampered by the low efficiency of tau aggregation, the requirement of high protein concentrations, and the lack of suitable detection methods. Here we report a quantitative assay system that permits monitoring of the assembly of PHFs in real time by the fluorescence of dyes such as thioflavine S or T. Using this assay, we evaluated parameters that influence the efficiency of filament formation. Disulfide-linked dimers of tau constructs representing the repeat domain assemble into PHFs most efficiently, but other tau isoforms or constructs form bona fide PHFs as well. The rate of assembly is greatly enhanced by polyanions such as RNA, heparin, and notably polyglutamate which resembles the acidic tail of tubulin. The assembly is optimal at pH ~6 and low ionic strengths (<50 mM) and increases steeply with temperatures above 30 °C, indicating that it is an entropy-driven process.

Alzheimer's disease is characterized by two pathological protein deposits, the amyloid plaques, consisting largely of amyloid fibers assembled from the Aβ peptide (a derivative of the membrane protein APP, reviewed in ref *1*), and the neurofibrillary tangles which are bundles of paired helical filaments whose main constituent is the microtubule-associated protein tau (for review, see ref *2*). The unchecked precipitation of these aggregates in critical brain areas is believed to be partly responsible for the neuronal degeneration, and the disease has been classified into several stages on the basis of the spreading of neurofibrillary deposits (*3*). It is therefore important to understand the factors underlying the abnormal aggregation of Aβ and tau. Both form filaments that are ~10 nm wide; in the case of Aβ, they are smooth, while most tau filaments from Alzheimer brains show a characteristic "paired helical" structure, resembling two strands wound around one another, with a crossover periodicity of ~80 nm and widths varying between 10 and 20 nm (reviewed in ref *4*).

The Aβ peptide shows a high tendency to form fibers with a cross-β-substructure (*5*, *6*). Its assembly mechanism has been studied with a number of different methods, such as electron microscopy, turbidity, sedimentation, fluorescence, or birefringence following the binding of dyes such as Congo red, thioflavine T (ThT[1]), or thioflavine S (ThS), and others (reviewed in ref *7*). This work resulted in a detailed kinetic model based on seeded assembly (*8*, *9*).

By contrast, tau is a highly soluble protein (as shown by its stability toward heat or acid treatment). Thus, it shows hardly any tendency to aggregate under physiological buffer conditions. Soluble tau protein contains very little secondary structure (no a, little b), and the same holds for Alzheimer PHFs, despite their long-range periodicity (*10*). It is therefore not obvious why tau should aggregate in a specific manner, and which structural principle could be responsible for this. Progress in understanding the mechanism has been correspondingly slow. The problem was compounded by the difficulty of distinguishing bona fide Alzheimer-like PHFs from other types of aggregates. Several authors found that microtubule-associated proteins (MAPs), including tau, can form thin fibers under certain conditions (*11*−*14*), but these often had a smooth appearance so that the relationship with Alzheimer PHFs remained uncertain. In our work, we have therefore searched for assembly conditions that would generate the ultrastructural phenotype of Alzheimer PHFs, as judged by electron microscopy. Several factors supporting assembly emerged in recent years. (1) The repeat domain of tau forms PHFs more readily than full-length tau isoforms (*15*). (2) Assembly proceeds more rapidly if the protein subunits are cross-linked into dimers, e.g., by an oxidized disulfide bridge at Cys322 (*15*, *16*), suggesting that dimers are important building blocks for PHFs. (3) Polyanions further enhance the efficiency of assembly, presumably by compensating for the positive charges of tau in a coacervate-like fashion. This can be achieved by extracellular components such as heparin (*17*, *18*) or intracellular factors such as RNA (*19*) or polyglutamate (as shown here).

These improvements made it possible to develop an assay to monitor PHF assembly in real time, and at physiological protein concentrations. Here we describe the fact that thioflavine dyes which can be used to stain amyloid-like deposits and neurofibrillary tangles in postmortem brains (*20*−*22*) can be used to quantify the formation of paired

† This project was supported by a grant from the Deutsche Forschungsgemeinschaft.

* Corresponding author. Telephone: +49-40-89982810. Fax: +49-40-89716822. E-mail: mandelkow@mpasmb.desy.de.

[1] Abbreviations: PHFs, paired helical filaments; ThS, thioflavine S; ThT, thioflavine T.

S0006-2960(98)00537-6 CCC: $15.00
Published on Web 06/24/1998

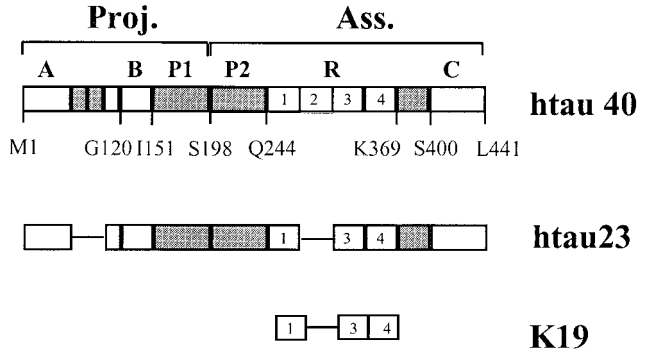

FIGURE 1: Bar diagram of tau isoforms and constructs. From top to bottom are htau40 (the longest human isoform of tau in the human central nervous system; *28*), htau23 [the shortest isoform, lacking the two near-N-terminal inserts (gray) and the second repeat], and construct K19, containing only repeats 1, 3, and 4. The N-terminal part is termed the "projection domain" and the C-terminal part the "assembly domain" because it binds to microtubules and promotes their assembly. This domain contains three or four repeats (~31 residues each) and the basic and proline-rich flanking domains (gray). The repeats form the core of Alzheimer PHFs. For details on the domain structure, see ref *25*.

helical filaments in solution. We demonstrate that this assay is a sensitive tool for monitoring the kinetics of filament assembly under different conditions, and we use it to determine the influence of parameters such as temperature, ionic strength, subunit dimerization, domain composition, and others. The results show that tau dimers are important for PHF formation under all conditions tested so far, that the interaction with the dyes depends on the polymeric form of tau, and that PHF assembly is entropy-driven and occurs at low ionic strengths and physiological pH. Surprisingly, polyglutamate can drive tau into assembly of PHFs. This may be significant since tau is normally bound to the C-terminal region of tubulin which is very rich in Glu residues and can be further acidified by enzymatic polyglutamylation (*23*). This opens the possibility that PHF assembly is initiated right on the microtubule surface to which the repeats of tau bind (*24*−*26*).

MATERIALS AND METHODS

Chemicals and Proteins. Heparin (average MW of 6000), poly-L-glutamate (average MW of 1000), tRNA (from bovine liver), and thioflavine S and T were obtained from Sigma. Solvents for measurement of the dependence of thioflavine fluorescence on viscosity and dielectric constants were obtained from Merck except for ethylene glycol (Sigma) and glycerol (99.5%, Gerbu). Htau40, htau23, and construct K19 of tau protein (see Figure 1) were expressed in *Escherichia coli* as described (*27*). The numbering of the amino acids is that of the isoform htau40 containing 441 residues (*28*). The protein was expressed and purified as described elsewhere, making use of the heat stability and FPLC Mono S (Pharmacia) chromatography (*25*). The purities of the proteins were analyzed by SDS−PAGE. Protein concentrations were determined by the Bradford assay.

Preparation of Dimeric Tau. Dimers of tau isoforms or constructs were allowed to form by incubation at 10 mg/mL after removal of DTT. The dimers were separated from monomers by gel filtration on a Superdex 75 column (Pharmacia) equilibrated with 200 mM NH_4Ac (pH 7.0). Fractions were collected and assayed for dimeric K19 by 15% SDS−PAGE under nonreducing conditions.

PHF Assembly. Tau isoforms or tau constructs at various concentrations (typically in the range of 1−100 μM) in volumes of 20−500 μL were incubated at 37 °C in 50 mM NH4Ac (pH 7) or 20 mM MOPS/NaOH (pH 7.0) containing various anionic cofactors (RNA, polyglutamate, or heparin) at approximately equimolar or indicated concentrations. Incubation times varied from minutes up to several days. PHF formation was always confirmed by electron microscopy. For evaluation of the thioflavine fluorescence assay, filamentous protein was separated from soluble protein by centrifugation at 100000*g* for 1 h and quantified using a Bradford assay.

Electron Microscopy. Protein solutions diluted to 1−10 μM protein were placed on 600-mesh carbon-coated copper grids for 1 min and negatively stained with 2% uranyl acetate for 45 s. The specimens were examined under a Philips CM12 electron microscope at 100 kV.

Fluorescence Spectroscopy. Fluorescence was measured at 22 °C with a Spex Fluoromax instrument (Spex Instruments SA) with excitation at 440 nm and emission at 480 or 500 nm. Excitation and emission slit widths were set to 5 nm (1.175 mm). Measurements were carried out at room temperature in 50 mM ammonium acetate (pH 6.5) or 20 mM Na/MOPS (pH 6.5) with 5 μM ThS or ThT unless otherwise stated. Background fluorescence and light scattering of the sample without thioflavine were subtracted when needed.

Solvent Dependence of Thioflavine Fluorescence. The solvent dependence of fluorescence intensity and the emission maxima for ThS and ThT were investigated by using solvents or binary solvent systems with varying dielectric constants and viscosities. Fluorescence emission spectra of thioflavine dyes at 10 μM were recorded at 25 °C with excitation at 440 nm. Values for dielectric constants and viscosities of various solvents were taken from the literature (*29*, *30*).

RESULTS

(a) Formation of PHFs Can Be Induced by Several Polyanions. The assay for the assembly of PHFs in solution was initially developed using short tau constructs such as K19 (Figure 1) comprising the repeat domain only (*31*). We used a construct of three repeats because it polymerizes most efficiently (*15*). Furthermore, since dimerization of tau is required for PHF formation (*16*), we started filament formation with the dimeric form of the protein, cross-linked via the single Cys322. In the absence of polyanions, K19 will only form filaments after long incubation times at very high protein concentrations (>100 h and 2 mM; see ref *19*), but coassembly with polyanions reduces this to the range of hours and close to the physiological range of tau (1−10 μM; see below). We used three types of polyanions, heparin (following refs *17* and *18*), tRNA (*19*), or polyglutamate. In the case of full-length tau isoforms, the assembly into PHFs could be induced by polyanions in a similar fashion, but generally it remained slower and required higher concentrations since the N- and C-terminal domains of tau act as inhibitors of assembly.

Typical filaments of htau23 or construct K19 are shown in Figure 2. They have the twisted appearance with a width of 10−20 nm and a periodicity around 80 nm regardless of the polyanion used. Electron microscopy was an essential

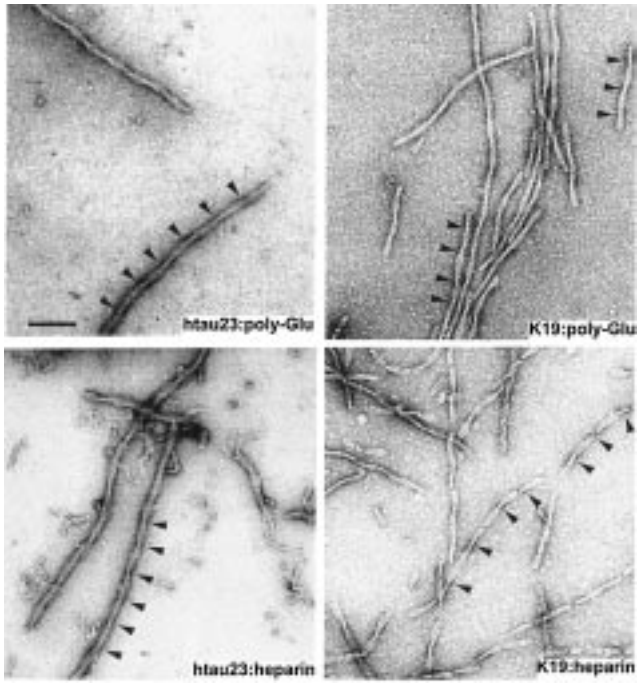

FIGURE 2: Electron micrographs and fluorescence microscopy of in vitro PHFs. Filaments were made from the following combinations of tau and polyanions: htau23 and polyglutamate (top left), htau23 and heparin (bottom left), K19 and polyglutamate (top right), and K19 and heparin (bottom right). The bar corresponds to 100 nm. Crossover periodicities (~80 nm) are indicated by arrowheads.

part of the experiments because under some conditions tau can form aggregates of a different appearance whose relationship to Alzheimer PHFs remains to be established (*11*, *13*, *32*, *33*). There were differences in the rate of filament formation (heparin > RNA > polyglutamate, in decreasing efficiency), and some polyanions even failed to induce filament formation under our conditions (notably DNA; data not shown). Nevertheless, we conclude that members of all physiologically relevant classes of polyanions (polycarboxylates, polyphosphates, and polysulfates) are capable of inducing PHFs. For the assembly assay in solution, we focused on heparin or polyglutamate, as both types of polyanions were efficient and represent different chemical structures (sugar and sulfate vs peptide and carboxylate). RNA could not be used for the fluorescence-based assay since, like DNA, it increases the fluorescence of the reporter molecule ThT or ThS significantly (*34*, *35*) so that the extent of filament formation cannot be quantified.

(b) Assembly of PHFs Can Be Monitored by the Interaction with Fluorescent Thioflavine Dyes. Neurofibrillary tangles in Alzheimer's disease brains can be detected by ThS or ThT, and PHFs obtained ex vivo or in vitro can also be stained with these dyes (*16*, *22*, *36*). We therefore asked whether they can be used for a quantitative assay for filament formation. Furthermore, we looked for differences between ThS and ThT since the latter one often is used to quantify amyloid formation in vitro (*37*−*39*). Figures 3 and 4 show that filaments formed from tau in the presence of polyanions can indeed be quantified using these fluorescent dyes. In Figure 3, excitation and emission spectra of the free dyes and of those in the presence of PHFs assembled in vitro are shown. Both dyes show changes in excitation and emission spectra upon binding to PHFs (Figure 3). At an excitation wavelength of 440 nm, the spectrum of ThT shows no change

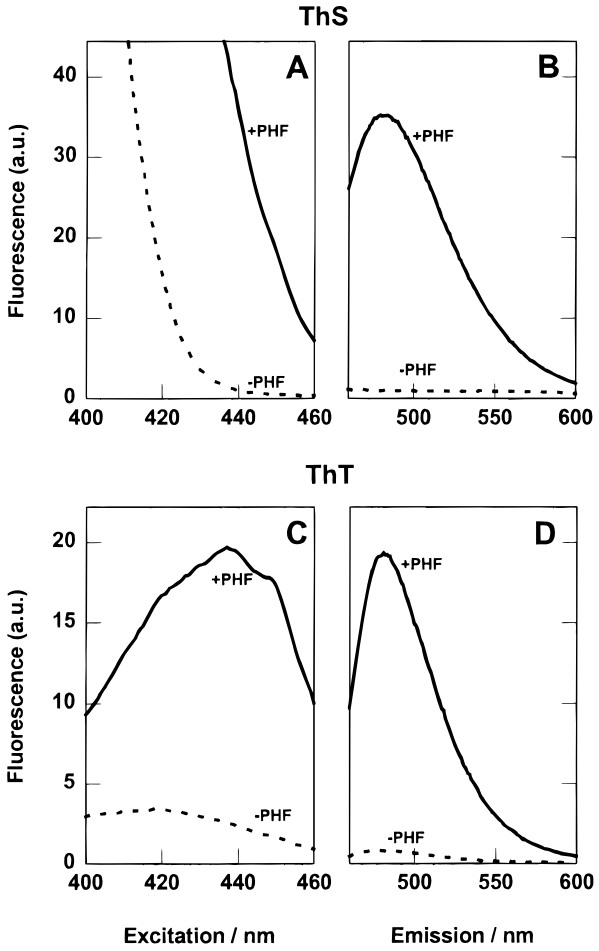

FIGURE 3: Thioflavine dyes are sensitive to the assembly of PHFs. ThS at 5 μM (A and B) and ThT at 5 μM (C and D) were incubated in 50 mM ammonium acetate (pH 7.0) without (dashed) or with 2 μM (monomer units) K19 filaments (solid) formed in the presence of heparin. (A and C) Excitation spectra with the emission wavelength at 480 nm. (B and D) Emission spectra with the excitation wavelength at 440 nm. Note that the fluorescence intensity at 480 nm increases 35-fold (A and B) or 25-fold (C and D) in the presence of filaments compared to that with the free dye. Fluorescence values are relative to the emission of 5 μM ThS at 480 nm.

in the emission maximum while that of ThS undergoes a blue shift from 550 to 480−490 nm. In the presence of 2 μM tau construct, K19 assembled into filaments the fluorescence intensity increases about 35-fold for ThS and 25-fold for ThT (excitation at 440 nm and emission at 480 nm). These factors are comparable to those obtained with amyloid fibrils formed from Aβ(1−40) or Aβ(1−42) (*38*). Importantly, neither component alone (protein or polyanion) or mixed immediately before the measurement at the fluorescence assay concentration has any significant effect on the excitation or emission spectra of the dyes (data not shown). Thus, these dyes are suitable for detecting the filamentous form of tau protein.

Next we determined the concentration range in which filaments can be quantified by thioflavine fluorescence. Increasing amounts of filaments were incubated at a constant concentration of dye (Figure 4A,B). The fluorescence increase for ThT (at 5 μM) is linear to at least 2.5 μM (monomer units) filamentous tau, and for ThS to ~4 μM, gradually reaching saturation at higher concentrations. Interestingly, ThT shows differences in fluorescence intensity

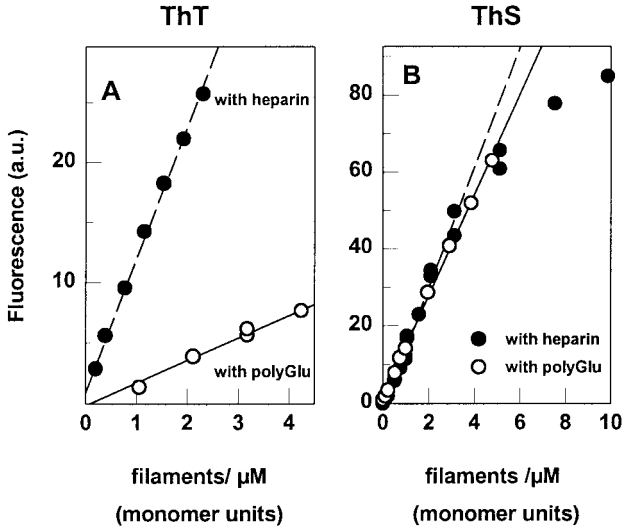

FIGURE 4: Standard curves for ThS and ThT fluorescence of in vitro filaments. Filaments were made from K19 (100 μM, corresponding to 1 mg/mL) in the presence of heparin (100 μM, ●) or polyglutamate (400 μM, ○). Varying amounts of filaments were incubated with 5 μM ThT (A) or 5 μM ThS (B). Excitation was at 440 nm.

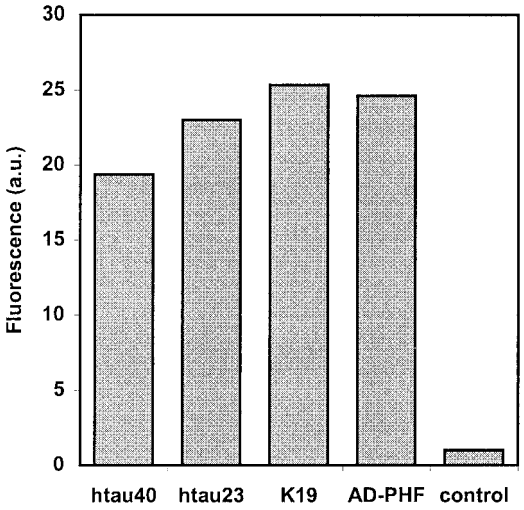

FIGURE 5: ThS fluorescence is a quantitative measure of PHFs. PHFs assembled from K19, htau23 or htau40 with heparin, or PHFs prepared from Alzheimer's disease brains were assayed for thioflavine fluorescence (5 μM ThS) at ~1 μM tau protein. Fluorescence values are relative to that of the free dye. The control value is for K19 with heparin mixed immediately before fluorescence measurement.

with regard to the polyanion used for polymerization of tau, being about 5-fold higher with heparin than with polyglutamate. Differences in fluorescence intensities have also been described for different amyloid fibrils (*37*, *38*). These were due to varying affinities for the dye, which is also true here (data not shown). Such differences were not observed with ThS. For convenience, we chose ThS in the following experiments for quantification of filaments.

(c) PHFs Assembled from Different Forms of Tau Show Comparable Thioflavine Fluorescence. PHFs assembled in vitro from either htau40, htau23, or K19 (see Figure 1) in the presence of heparin were polymerized, and then ThS fluorescence was measured at a 1 μM initial protein concentration. For comparison, authentic PHFs (comprising all six full-length isoforms) isolated from AD brain were also measured at 1 μM protein (monomer units) (Figure 5). All types of filaments showed comparable increases in thioflavine fluorescence, regardless of whether full-length tau or shorter constructs were used.

(d) Thioflavine T Behaves as a Molecular Rotor. Since the mechanism which underlies the increase and change in fluorescence of thioflavine dyes interacting with in vitro PHFs is not known, we measured emission spectra in different solvents with varying dielectric constants and viscosities. Remarkably, the dyes did show differences with respect to their dependence on solvent. Fluorophors often display an increase in intensity (quantum yield) and a blue shift upon decreasing solvent polarity (dielectric constant). Such a behavior is also seen for ThS (Figure 6A). Furthermore, the maximum emission wavelength is undergoing a classical blue shift with lower dielectric constants (data not shown). This is in contrast to ThT which shows no simple relationship between fluorescence intensity and dielectric constant (Figure 6A); moreover, changes in the emission maximum are negligible (data not shown). However, when the dependence on viscosity at a given dielectric constant is observed, a strong correlation is seen, with higher fluorescence intensities at higher viscosities (Figure 6B). The data could be fitted using the empirical relationship $F \propto \eta^{0.6}/\epsilon$. Such a relationship has been described previously for a class of fluorescent dyes called molecular rotors (*30*, *40*). These dyes show increased fluorescence when introduced into high-viscosity media due to the decreased torsional relaxation. Therefore, the increase in fluorescence intensity for ThS upon binding to filaments can be explained in terms of a decrease in polarity. From the emission maximum of 480−490 nm (depending on ThS concentration; data not shown), a local dielectric constant of less than 20 might be expected. For ThT only, a combination of a lower dielectric constant and changes in microviscosity upon binding to filaments accounts for the observed increase in fluorescence (see the Discussion below).

(e) Assembly of PHFs Is Optimal in the Presence of Stoichiometric Amounts of Polyanions. To determine the role of the polyanions in PHF formation in vitro, we investigated the influence of concentration and stoichiometry of tau and polyanions with respect to filament formation. As shown in Figure 7, the extent of filament formation depends on the absolute and relative concentrations of the two partners, tau and polyanion (shown for heparin in Figure 7A or polyglutamate in Figure 7B). Polyanions stimulate assembly even at low tau concentrations where assembly without polyanions would be hardly noticeable (e.g., 1−10 μM, Figure 7C or 9). However, filament formation decreases steeply beyond a heparin:tau ratio of >4:1 upon varying tau at a constant concentration of heparin (300 μM, Figure 7C). This is not due to the lower concentration of tau but rather to the increased ratio of polyanion to protein as can be seen by varying the protein concentration with equimolar concentrations of heparin. Here even at 10 μM protein, the formation of PHFs is much more efficient compared to that at 75 μM protein with 300 μM heparin. This indicates that PHF assembly proceeds via a complex of protein and polyanion at a defined stoichiometry and that excess polyanion is inhibitory. Independent of the relationships described above, tau assembly is always much slower (hours to days) if starting from monomeric solutions, consistent with earlier

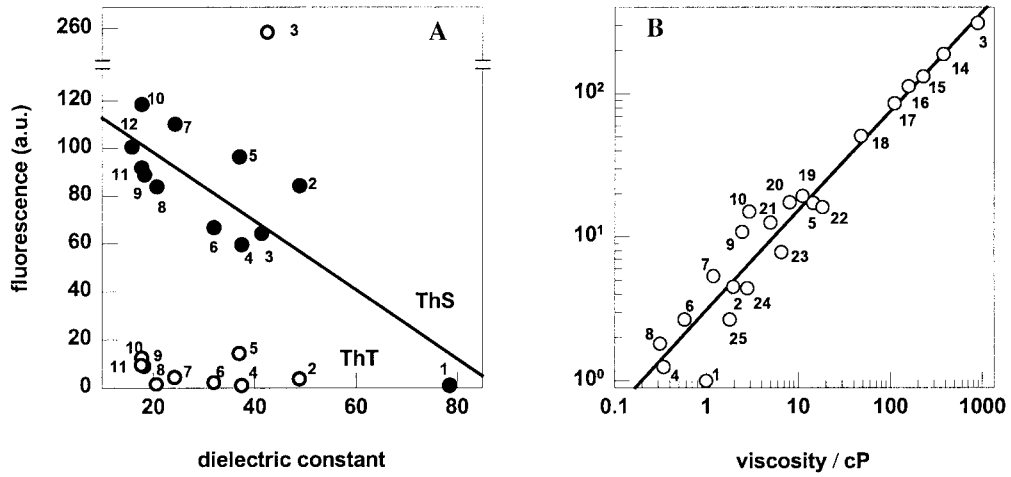

FIGURE 6: Dependence of thioflavine fluorescence on solvent polarity and viscosity. Fluorescence emission spectra (excitation at 440 nm) of ThT (○) or ThS (●) at 10 μM were measured in various solvents (see Materials and Methods) at 25 °C. ThS shows a strong dependence on the solvent polarity (dielectric) constant for emission intensity (A) and the emission wavelength maximum (data not shown), while ThT shows a strong dependence on the solvent viscosity for emission intensity (B) but no obvious dependence of emission maximum on solvent (data not shown): (1) water, (2) DMSO, (3) glycerol, (4) acetonitrile, (5) ethylene glycol, (6) methanol, (7) ethanol, (8) acetone, (9) 2-propanol, (10) 1-butanol, (11) 2-methyl-1-propanol, (12) 2-butanol, (13) methylene chloride, (14) ethylene glycol/glyercol (2:8, v/v), (15) ethylene glycol/glyercol (3:7, v/v), (16) ethylene glycol/glyercol (4:6, v/v), (17) ethylene glycol/glyercol (5:5, v/v), (18) ethylene glycol/glyercol (7:3, v/v), (19) ethylene glycol/2-propanol (7:3, v/v), (20) ethylene glycol/2-propanol (5:5, v/v), (21) ethylene glycol/2-propanol (3:7, v/v), (22) water/glyercol (1:3, v/v), (23) water/glyercol (1:1, v/v), (24) water/ethanol (1:1, v/v), and (25) water/methanol (1:1, v/v).

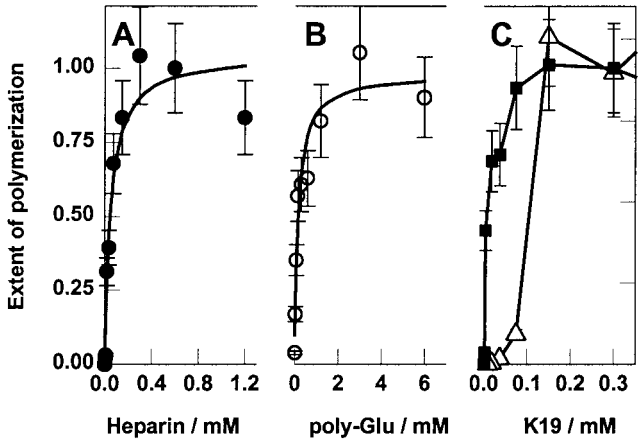

FIGURE 7: Tau and polyanions coassemble in stoichiometric amounts. Filaments were formed for 2 days at 37 °C with either a constant concentration of K19 (300 μM) and varying amounts of heparin (A) and polyglutamate (B) or varying amounts of protein with 300 μM heparin (C, △) or at 1:1 protein:heparin (C, ■). The extent of polymerization was determined by using ThS. Note the extent of polymerization is dependent on the amount of polyanion. At low protein concentrations, excess polyanion inhibits the kinetics of filament formation (C). However, it should be noted that after 2 weeks even in the presence of excess heparin filaments are observed.

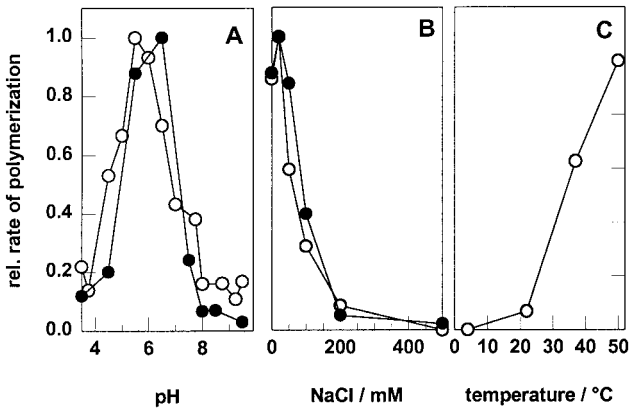

FIGURE 8: Dependence of filament formation on pH, NaCl concentration, and temperature. The rate of filament formation from K19 (60 μM) in the presence of heparin (60 μM, ●) or polyglutamate (240 μM, ○) was monitored with ThS with variation of either pH (A), NaCl concentration (B), or temperature (C). For convenience, values are normalized to maximum values for each curve. The absolute rate in the presence of heparin (1 μM/min) is ~4 times higher than that with polyglutamate. Note that the pH optimum is around 6, that the ionic strength optimum is below 50 mM, and that elevated temperatures are favorable for PHF formation.

observations (*16*). It was therefore important to start with solutions of tau dimers since the dimers appear to be effective building blocks of PHFs under a wide range of conditions (see Figure 10). Especially when low protein concentrations are used, the kinetics of dimerization becomes rate limiting (data not shown).

(f) PHF Assembly Is Optimal at pH ~6, Low Salt Concentrations, and Elevated Temperatures. Next we examined the dependence of filament formation on conditions such as buffer, ionic strength, and temperature. In Figure 8A, the pH dependence of filament formation has an optimum around pH 6. In all cases, the formation of bona fide PHFs was assured by electron microscopy. The pH optimum of around 6 may point to an involvement of histidine residues (pK = 6) in the process of filament formation. Furthermore, the formation of PHFs is highly sensitive to elevated ionic strength and decreases steeply above 50 mM NaCl, in the presence of either polyglutamate or heparin (Figure 8B). This points toward the ionic character of the interaction between tau with these polyanions which would be shielded by salts. The temperature dependence of filament formation is remarkable in that it is extremely slow below 20 °C and then increases steeply (and almost linearly) between ~20 and 50 °C (Figure 8C). The fact that PHFs can be formed de novo even at 50 °C (and probably beyond) shows that the properties of tau are not influenced by harsh treatment. This is consistent with the "natively unfolded" state of tau described earlier (*10*) which

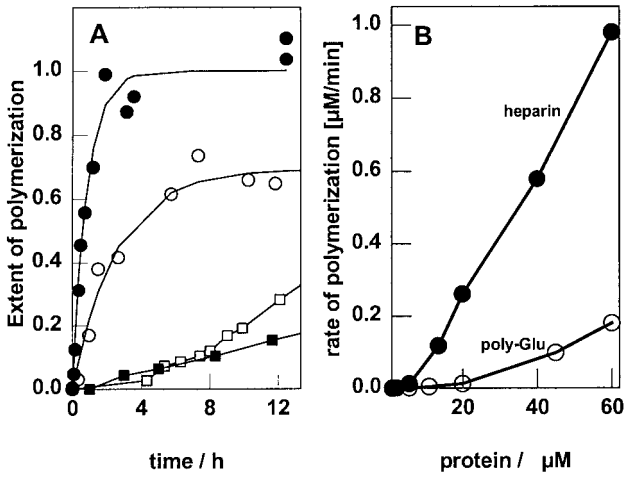

FIGURE 9: The time course of filament formation can be monitored by thioflavine fluorescence. Filament formation of K19 in the presence of heparin or polyglutamate monitored by ThS: (A) K19 (40 μM) and 40 μM heparin (●), K19 (2 μM) and 2 μM heparin (■), K19 (40 μM) and 240 μM polyglutamate (○), and K19 (10 μM) and 60 μM polyglutamate (□) in 50 mM NH_4Ac at pH 7.0 and 37 °C. Time courses with 40 μM K19 are fitted to a single-exponential function, while this was not possible for the lower protein concentrations. (B) Maximum velocity of filament formation at different protein concentrations. The concentration of K19 was varied between 1 and 60 μM in the presence of heparin (1:1, ●) or polyglutamate (6:1, ○). At low concentrations of protein, a lag phase becomes apparent, and therefore, maximum velocities were used instead of initial velocities.

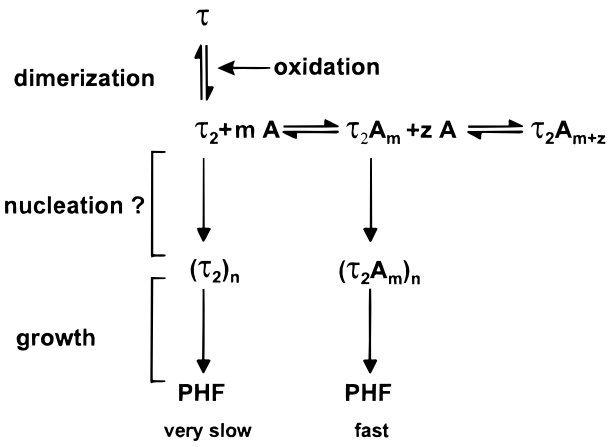

FIGURE 10: Model of PHF assembly. PHF formation requires the dimerization of tau monomers (τ) possibly via a disulfide linkage at Cys322. Dimers (τ_2) of tau can form PHFs only very slowly. In the presence of polyanion (A), tau forms a complex (τ_2A_m) which will assemble very fast into PHFs. Excess polyanion, however, will form a complex with tau with another stoichiometry (τ_2A_{m+z}) which is assembly incompetent. The lag phase during polymerization that is visible in certain experiments could be due to a rate-limiting nucleation step.

allows even boiled and acid-treated tau to interact productively with microtubules.

(g) PHFs Can Aggregate Rapidly at Physiological Concentrations of Tau. An important criterion for judging whether the assembly conditions in vitro could reflect cellular events is the concentration dependence. The cellular concentration is on the order of about micromolar or less (*41*, *42*), while our earlier PHF assembly experiments required 50−100-fold higher concentrations (*15*). Figure 9 shows time courses of filament formation monitored by thioflavine fluorescence in a physiological concentration range of tau. Most curves can be fitted to a single-exponential function at high concentrations of protein (>10 μM K19 with heparin, >40 μM with polyglutamate). The time course of assembly is compatible with a simple elongation model of the type $P_n + S \rightarrow P_{n+1}$ (*43*).

At lower tau concentrations, the relative rate of filament formation is decreasing and a lag phase becomes apparent. In the presence of heparin and polyglutamate, this is observed at protein concentrations below ~2 and 10 μM, respectively (Figure 9). A lag phase is more prominent at higher salt concentrations or with an increased ratio of heparin to protein (data not shown). This is not due to lower specific fluorescence of the dye for short filaments or oligomers, since during the lag phase few but long (several of 100 nm) filaments are observed in the electron microscope (data not shown). This suggests that nucleation becomes rate-limiting as has been shown to be the case for β amyloid formation (*8*).

DISCUSSION

PHF formation is one of the critical steps in Alzheimer's disease and one of the important pathological hallmarks. It is, however, not clear what triggers the transformation of the highly soluble tau protein into insoluble filaments. Many different factors have been implicated in this process, primarily on the basis of the fact that these factors were found to be associated with neurofibrillary tangles (e.g., kinases and ubiquitin; see refs *44* and *45*) or that modifications of the tau protein itself occurred within PHFs (e.g., phosphorylation, glycation, or proteolysis; *46*−*48*). To better understand of the role of these factors in PHF formation, one needs a qualitative and quantitative measure for filament formation that is applicable in solution and in real time. Precipitation assays, turbidity measurements, and electron microscopy have been employed in analyzing filament formation (*10*−*19*, *33*, *49*−*52*). However, thus far, no kinetic or quantitative analysis for filament formation has been performed due to the difficulties in inducing tau to polymerize despite its high solubility. In principle, the same methods used to investigate the self-assembly of cytoskeletal or amyloid filaments should be applicable to investigations of PHF formation in vitro (for reviews, see refs *7* and *43*). In all cases, the key problem is to induce polymerization efficiently and to obtain a reliable signal for the degree of assembly.

Here we report the use of thioflavine dyes for a quantitative analysis of filament formation from tau protein. As in the case of amyloid fibrils, these dyes only stain proteins in the fibrous polymerized form. It is often stated that the binding and increase in thioflavine fluorescence are specific for the cross-β-structure typical of amyloid fibers (*38*). However, this is not necessarily true for the interaction of thioflavine with other partners which are devoid of cross-β-structure; examples are PHFs or DNA (*10*, *34*). The reason for the fluorescence intensity increase upon binding of thioflavine dyes to PHF is not known. Several possible alternatives (conformational changes, e.g., local β-conformation or formation of a dye binding site upon aggregation) are currently under investigation. Nevertheless, thioflavine dyes are suitable for monitoring the assembly of in vitro PHFs from tau protein in the presence of polyanions (Figure 3). We show here that filaments can be quantified using a

thioflavine assay (Figure 4) which is highly sensitive since it quantifies filament formation in a 0.1−4 μM range (monomer units). Using this assay, it is possible to determine parameters that influence the efficiency of filament formation (Figures 5 and 6). An important feature of polyanion-stimulated PHF formation is the apparent roughly equimolar stoichiometry (Figure 5) which implies a copolymerization of protein and polyanion. This is also supported by the finding that polyanions are found together with tau protein in a 100000*g* pellet in a near stoichiometric manner, while an excess of either component is found in the supernatant (data not shown). An excess of polyanions slows the kinetics of filament formation, presumably due to the formation of assembly incompetent complexes of tau and polyanion (Figure 10), but does not reduce the final extent of polymerization.

The efficiency of filament formation has a bell-shaped pH optimum (Figure 8A), with an optimum around pH 6. The pH profile is similar to that obtained by others for the formation of tau aggregation in the absence of polyanions (*13*, *53*). We note that tau contains four or five histidine residues in the repeat region (depending on isoform) which might be important for protein−polyanion and/or protein−protein interaction during filament formation. For Aβ amyloid formation, it has been shown that two histidine residues [His13 and His14 of Aβ(1−40)] are involved in the amyloid fiber formation but not in the formation of the amyloidogenic secondary structure (*54*). Alternatively, electrostatic repulsion at a pH below 4 or decreased binding of polyanion at higher pH might account for the observed pH optimum. To clarify this, a more detailed analysis would be required. At any rate, the pH profile shows that in principle filament formation is favorable at physiological pH. The salt concentration dependence of filament formation in the presence of polyanions (Figure 8B) clearly points to the ionic character of the interaction between tau and the polyanions since in the absence of polyanions filament formation from tau is only possible at elevated salt concentrations (*15*, *55*). Other authors have shown that in the presence of arachidonic acid filament formation from tau protein is inhibited at elevated NaCl concentrations (>200 mM; *56*). A similar salt concentration dependence for filament formation in the absence of polyanions has also been reported (*13*). In these experiments, a mixture of phosphorylated and nonphosphorylated tau protein has been used, and it is still uncertain whether the tau−tau interaction is influenced by phosphorylation. Finally, the strong temperature dependence of filament formation (Figure 8C) is remarkable and suggests that the molecular interactions on which PHFs are based must be rather stable. It also shows that the polymerization reaction is entropy-driven. Such a behavior could be caused either by hydrophobic interactions or by specific ionic interactions, but not, for example, by nonspecific ionic strength effects or H bonds (*57*). Given the highly charged nature of tau, the temperature dependence of PHF assembly may be dominated by ionic interactions, but this issue needs further substantiation.

The time courses of filament formation shown in Figure 9 reveal that at elevated protein concentrations filament assembly follows a single-exponential function and may therefore be described by a simple kinetic mechanism of endwise subunit addition ($P_n + S \rightarrow P_{n+1}$). However, under certain condition, e.g., low protein concentration, a lag phase becomes apparent during the initial phase of assembly. The presence of this lag phase suggests that formation of a polymerization nucleus larger than a tau dimer becomes rate-limiting, a feature also known for other polymerization processes for microtubules (*58*) or amyloid fibers (*8*). In developing the assembly assay, we initially started with a tau construct (K19) comprising only repeats 1, 3, and 4. This choice was made because (1) PHF assembly proceeds most easily from the repeat domain (*15*), (2) the core of Alzheimer PHFs are largely made up of the repeat domain of tau (*36*, *59*), (3) dimerization is an important requirement for filament formation in vitro (*16*), and (4) it had been shown that truncation of tau precedes filament formation in vivo (*60*). However, larger tau constructs and tau isoforms can be assembled into PHFs as well and monitored in the same fashion. The main difference is that the domains outside the repeats, especially the more acidic N-terminal domain, make filament formation less efficient so that higher concentrations and/or longer times are required. Apart from that, the general characteristics (appearance of PHFs, interactions with polyanions, and dependence on pH, salt concentration, and temperature) are very similar. The diagram in Figure 10 summarizes the steps in PHF assembly known thus far.

Tau from Alzheimer PHFs occurs in an abnormal state of phosphorylation, and it is generally thought that phosphorylation plays a role in generating a "pathological conformation" of tau or preparing the ground for PHF assembly by detaching tau from microtubules (for reviews, see refs *61*−*63*). The experiments described here were carried out with unphosphorylated recombinant tau expressed in *E. coli*. This means that phosphorylation is not absolutely necessary for PHF assembly in vitro, although one cannot exclude a helper function in cells. This problem will be addressed in future experiments.

A final point concerns the nature of the polyanion used to enhance PHF assembly. It was noted recently that heparin or heparan sulfate potently stimulates the assembly of tau (*17*, *18*, *64*). To put this into a physiological context, these authors discussed the possibility that extracellular polysulfates might enter the cytosol and thus nucleate Alzheimer PHFs in aging neurons. While the strong effect of heparin is unambiguous in vitro, we would argue that other polyanions residing in the cytosol are more likely to play a role in vivo. The prominent cytosolic polyanions are polyphosphates such as RNA, or polycarboxylates (e.g., acidic peptides or protein domains rich in Glu or Asp). We showed earlier that RNA indeed is capable of stimulating PHF assembly from tau and in competing with microtubules for tau or other MAPs (*19*). We have now extended this to acidic peptides such as polyglutamate. Although polyglutamate is less potent than heparin or RNA, it is particularly intriguing. Tau and its natural partner tubulin interact via the repeat region of tau (*24*−*26*) and the acidic C terminus of tubulin which can be further acidified by polyglutamylation (*65*). Therefore, it would be conceivable that in vivo PHFs are initiated on the surface of microtubules or that a proteolyzed acidic C terminus of tubulin induces tau aggregation. These possibilities of a microtubule-based assembly mechanism for PHFs are currently being studied.

ACKNOWLEDGMENT

We are grateful to K. Alm for expert technical assistance, to J. Biernat for providing tau constructs, and to T. Kampers for help with electron microscopy. AD PHFs were kindly provided by Dr. Peter Davies.

REFERENCES

1. Selkoe, D. J. (1996) *J. Biol. Chem. 271*, 18295−18298.
2. Friedhoff, P., and Mandelkow, E. (1998) in *Guidebooks to the Cytoskeletal and Motor Proteins and to the Extracellular Matrix and Adhesion Proteins* (Kreis, T., and Vale, R., Eds.) Oxford University Press, Oxford, U.K.
3. Braak, H., and Braak, E. (1997) *Neurobiol. Aging 18*, 351−357.
4. Crowther, R. A. (1993) *Curr. Opin. Struct. Biol. 3*, 202−206.
5. Kirschner, D. A., Abraham, C., and Selkoe, D. J. (1986) *Proc. Natl. Acad. Sci. U.S.A. 83*, 503−507.
6. Inouye, H., Fraser, P. E., and Kirschner, D. A. (1993) *Biophys. J. 64*, 502−519.
7. Harper, J., and Lansbury, P. J. (1997) *Annu. Rev. Biochem. 66*, 385−407.
8. Jarrett, J. T., and Lansbury, P. T. (1993) *Cell 73*, 1055−1058.
9. Lomakin, A., Teplow, D. B., Kirschner, D. A., and Benedek, G. B. (1997) *Proc. Natl. Acad. Sci. U.S.A. 94*, 7942−7947.
10. Schweers, O., Schönbrunn-Hanebeck, E., Marx, A., and Mandelkow, E. (1994) *J. Biol. Chem. 269*, 24290−24297.
11. Degarcini, E. M., Carrascosa, J. L., Correas, I., Nieto, A., and Avila, J. (1988) *FEBS Lett. 236*, 150−154.
12. Wille, H., Mandelkow, E. M., and Mandelkow, E. (1992) *J. Biol. Chem. 267*, 10737−10742.
13. Wilson, D. M., and Binder, L. I. (1995) *J. Biol. Chem. 270*, 24306−24314.
14. Zhang, E. Y., Deture, M. A., Bubb, M. R., Caviston, T. L., Erdos, G. W., Whittaker, S. D., and Purich, D. L. (1996) *Biochem. Biophys. Res. Commun. 229*, 176−181.
15. Wille, H., Drewes, G., Biernat, J., Mandelkow, E. M., and Mandelkow, E. (1992) *J. Cell Biol. 118*, 573−584.
16. Schweers, O., Mandelkow, E. M., Biernat, J., and Mandelkow, E. (1995) *Proc. Natl. Acad. Sci. U.S.A. 92*, 8463−8467.
17. Goedert, M., Jakes, R., Spillantini, M. G., Hasegawa, M., Smith, M. J., and Crowther, R. A. (1996) *Nature 383*, 550−553.
18. Perez, M., Valpuesta, J. M., Medina, M., Degarcini, E. M., and Avila, J. (1996) *J. Neurochem. 67*, 1183−1190.
19. Kampers, T., Friedhoff, P., Biernat, J., and Mandelkow, E. M. (1996) *FEBS Lett. 399*, 344−349.
20. Wisniewski, H. M., Wen, G. Y., and Kim, K. S. (1989) *Acta Neuropathol. 78*, 22−27.
21. Yen, S. H., Gaskin, F., and Terry, R. D. (1981) *Am. J. Pathol. 104*, 77−89.
22. Roher, A., Palmer, K., Chau, V., and Ball, M. (1988) *J. Cell Biol. 107*, 2703−2716.
23. Boucher, D., Larcher, J. C., Gros, F., and Denoulet, P. (1994) *Biochemistry 33*, 12471−12477.
24. Butner, K. A., and Kirschner, M. W. (1991) *J. Cell Biol. 115*, 717−730.
25. Gustke, N., Trinczek, B., Biernat, J., Mandelkow, E. M., and Mandelkow, E. (1994) *Biochemistry 33*, 9511−9522.
26. Goode, B. L., Denis, P. E., Panda, D., Radeke, M. J., Miller, H. P., Wilson, L., and Feinstein, S. C. (1997) *Mol. Biol. Cell 8*, 353−365.
27. Biernat, J., Mandelkow, E. M., Schröter, C., Lichtenberg-Kraag, B., Steiner, B., Berling, B., Meyer, H. E., Mercken, M., Vandermeeren, A., Goedert, M., and Mandelkow, E. (1992) *EMBO J. 11*, 1593−1597.
28. Goedert, M., Spillantini, M., Potier, M., Ulrich, J., and Crowther, R. (1989) *EMBO J. 8*, 393−399.
29. Weast, R. C., and Astle, M. J. (1981) *CRC Handbook of Chemistry and Physics*, CRC Press Inc., Boca Raton, FL.
30. Kung, C. E., and Reed, J. K. (1986) *Biochemistry 25*, 6114−6121.
31. Lee, G., Neve, R. L., and Kosik, K. S. (1989) *Neuron 2*, 1615−1624.
32. Lichtenberg-Kraag, B., and Mandelkow, E. M. (1990) *J. Struct. Biol. 105*, 46−53.
33. Alonso, A. D., Grundke-Iqbal, I., and Iqbal, K. (1996) *Nat. Med. 2*, 783−787.
34. Canete, M., Villanueva, A., Juarranz, A., and Stockert, J. C. (1987) *Cell. Mol. Biol. 33*, 191−199.
35. Parker, C. A., and Joyce, T. A. (1973) *Photochem. Photobiol. 18*, 467−474.
36. Wischik, C., Novak, M., Thogersen, H., Edwards, P., Runswick, M., Jakes, R., Walker, J., Milstein, C., Roth, M., and Klug, A. (1988) *Proc. Natl. Acad. Sci. U.S.A. 85*, 4506−4510.
37. Naiki, H., Higuchi, K., Hosokawa, M., and Takeda, T. (1989) *Anal. Biochem. 177*, 244−249.
38. LeVine, H. (1993) *Protein Sci. 2*, 404−410.
39. Naiki, H., and Nakakuki, K. (1996) *Lab. Invest. 74*, 374−383.
40. Loutfy, R. O., and Arnold, B. A. (1982) *J. Phys. Chem. 86*, 4205−4211.
41. Drubin, D., and Kirschner, M. (1986) *J. Cell Biol. 103*, 2739−2746.
42. Drubin, D., Reinstein, S., Shooter, E., and Kirschner, M. (1985) *J. Cell Biol. 101*, 1799−1807.
43. Oosawa, F., and Asakura, S. (1975) *Thermodynamics of the polymerisation of protein*, Academic Press, London.
44. Vincent, I. J., and Davies, P. (1992) *Proc. Natl. Acad. Sci. U.S.A. 89*, 2878−2882.
45. Morishima-Kawashima, M., Hasegawa, M., Takio, K., Suzuki, M., Titani, K., and Ihara, Y. (1993) *Neuron 10*, 1151−1160.
46. Novak, M., Jakes, R., Edwards, P. C., Milstein, C., and Wischik, C. M. (1991) *Proc. Natl. Acad. Sci. U.S.A. 88*, 5837−5841.
47. Ledesma, M. D., Bonay, P., Colaco, C., and Avila, J. (1994) *J. Biol. Chem. 269*, 21614−21619.
48. Morishima-Kawashima, M., Hasegawa, M., Takio, K., Suzuki, M., Yoshida, H., Titani, K., and Ihara, Y. (1995) *J. Biol. Chem. 270*, 823−829.
49. Crowther, R. A., Olesen, O. F., Smith, M. J., Jakes, R., and Goedert, M. (1994) *FEBS Lett. 337*, 135−138.
50. Ledesma, M. D., Medina, M., and Avila, J. (1996) *Mol. Chem. Neuropathol. 27*, 249−258.
51. Scott, C. W., Fieles, A., Sygowski, L. A., and Caputo, C. B. (1993) *Brain Res. 628*, 77−84.
52. Troncoso, J. C., Costello, A., Watson, A. L., and Johnson, G. V. W. (1993) *Brain Res. 613*, 313−316.
53. Wischik, C. M., Edwards, P. C., Lai, R. Y. K., Roth, M., and Harrington, C. R. (1996) *Proc. Natl. Acad. Sci. U.S.A. 93*, 11213−11218.
54. Soto, C., and Frangione, B. (1995) *Neurosci. Lett. 186*, 115−118.
55. Crowther, R. A., Olesen, O. F., Jakes, R., and Goedert, M. (1992) *FEBS Lett. 309*, 199−202.
56. Wilson, D. M., and Binder, L. I. (1997) *Am. J. Pathol. 150*, 2181−2195.
57. Timasheff, S. N. (1972) in *Proteins of biological fluids* (Peeters, H., Ed.) Vol. 20, pp 511−519, Pergamon Press.
58. Johnson, K. A., and Borisy, G. G. (1977) *J. Mol. Biol. 117*, 1−31.
59. Novak, M., Kabat, J., and Wischik, C. M. (1993) *EMBO J. 12*, 365−370.
60. Mena, R., Edwards, P. C., Harrington, C. R., Mukaetovaladinska, E. B., and Wischik, C. M. (1996) *Acta Neuropathol. 91*, 633−641.
61. Trojanowski, J., and Lee, V. M. Y. (1995) *FASEB J. 9*, 1570−1576.
62. Johnson, G. V., and Jenkins, S. M. (1996) *Alzheimer's Dis. Rev. 1*, 38−54.
63. Mandelkow, E., and Mandelkow, E. M. (1995) *Curr. Opin. Cell Biol. 7*, 72−81.
64. Hasegawa, M., Crowther, R. A., Jakes, R., and Goedert, M. (1997) *J. Biol. Chem. 272*, 33118−33124.
65. Edde, B., Rossier, J., Le Caer, J. P., Desbruyeres, E., Gros, F., and Denoulet, P. (1990) *Science 247*, 83−85.

BI980537D